

Neural Adaptive Control by State Space Regulator of Universal Charge for the Compensation of Active and Reactive Power

¹A. Bouanane and ²A. Chaker

¹Departement d'Electrotechnique, University Dr. Moulay Tahar, Saida, D'Algerie

²Departement de Genie Electrique, Enset d'Oran, EL Mnaouer, Oran, BP 1523, D'Algerie

Abstract: In the present study, researchers present the effectiveness of the controller's electrical power flow universal (Unified Power Flow Controller, UPFC) with the choice of a control strategy. To evaluate the performance and robustness of the system, we proposed a hybrid control combining the concept of neural networks with conventional regulators vis-a-vis the changes in characteristics of the transmission line in order to improve the stability of the electrical power network.

Key words: UPFC system, adaptive control, Neural Networks State Space (SSNN), strategy, stability, Algerie

INTRODUCTION

With the rapid development of the modern world, the demand for electricity is growing and electrical installations are continually enhanced to meet these requirements. The construction of new plants and new lines are necessary but with FACTS devices, we can solve some problems while using the existing facilities.

Having highlighted the need for rapid control of power flow in transmission line and the description of the new concept of FACTS that was born to meet the increasing difficulties in networks including control of the flow on the axes transport, we are interested in the research to the controller's electrical power flow universel (Papic *et al.*, 1997; Song and Johns, 1999), Unified Power Flow Controller (UPFC).

The UPFC consists of two switching converter (series and shunt) (Fig. 1) and even this device is the union of a parallel compensator and a series compensator. It is capable of simultaneously and independently control the active power and reactive power. It can control the three parameters associated with power flow the line voltage, the impedance of the line and angle of transport.

Configuration variable universal charge (UPFC): It is assumed that the UPFC (Gyugyi, 1992) shown in Fig. 1 was plugged into a simplified transmission system, the arrival of the transmission line (Receiving end). The two voltage source inverters constituting the UPFC are connected together through a common DC circuit.

Two transformers T1 and T2 are used to connect the two inverters, one serial and one parallel to the transmission line. After all, this composition

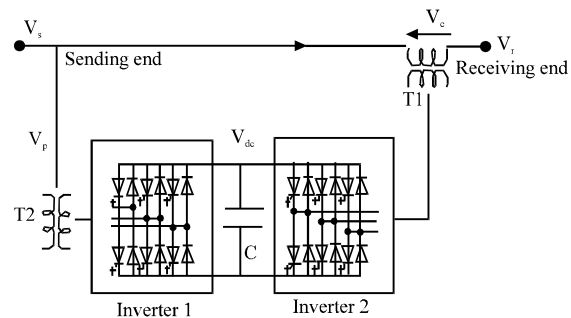


Fig. 1: UPFC system configuration

offers the UPFC's ability to control the active power and reactive power regardless of where:

- The series inverter (2) Inverter 2 performs the principal function of the UPFC by injecting an AC voltage in series (AC) with an amplitude and a phase angle adjustable
- The parallel UPS (1) Inverter 1 role is to provide or absorb the real power demanded by the inverter (2) to the connection (DC) as it can also produce or absorb reactive power according to demand and provide independent shunt compensation transmission line
- The series inverter (2) provides or absorbs the needed reactive power locally produced active power as a result of injecting a voltage in series

Modelling of the system UPFC: The simplified circuit of the control system and compensation of UPFC is shown in Fig. 2 modeling of this circuit is based on simplifying

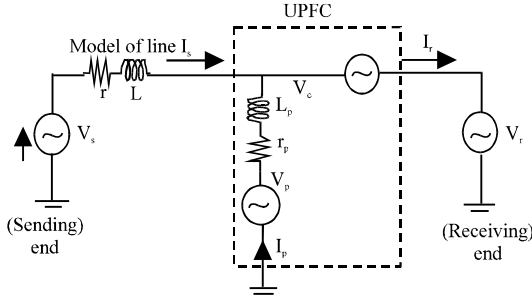


Fig. 2: Equivalent circuit of UPFC

assumptions in the form of ideal voltage sources then the dynamic equations of the UPFC are divided into three systems of equation, the equations of the series branch, the equations of parallel branch and those of the DC circuit. By applying Kirchhoff laws, researchers will have the following equations for each branch.

The modeling of the series branch is given by the following equations:

$$\begin{aligned} \frac{di_{sa}}{dt} &= -\frac{r}{L}i_{sa} + \frac{1}{L}(v_{sa} - v_{ca} - v_{ra}) \\ \frac{di_{sb}}{dt} &= -\frac{r}{L}i_{sb} + \frac{1}{L}(v_{sb} - v_{cb} - v_{rb}) \\ \frac{di_{sc}}{dt} &= -\frac{r}{L}i_{sc} + \frac{1}{L}(v_{sc} - v_{cc} - v_{rc}) \end{aligned} \quad (1)$$

The transformation of Park aims to model this three-phase system (a, b, c) two-phase (d, q) as follows:

$$\begin{bmatrix} x_d \\ x_q \\ x_0 \end{bmatrix} = \frac{2}{3} \begin{bmatrix} \cos(\omega t) & -\sin(\omega t) & 1/2 \\ \cos(\omega t - 120^\circ) & -\sin(\omega t - 120^\circ) & 1/2 \\ \cos(\omega t + 120^\circ) & -\sin(\omega t + 120^\circ) & 1/2 \end{bmatrix}^T \begin{bmatrix} x_a \\ x_b \\ x_c \end{bmatrix} \quad (2)$$

where, x can be a voltage or current. In the case, the component x0 is not seen as the power system is assumed to be symmetric.

After the transformation of Park, Eq. 1 is expressed in the d_q reference by the equations:

$$\begin{aligned} \frac{di_{sd}}{dt} &= \omega i_{sq} - \frac{r}{L}i_{sd} + \frac{1}{L}(v_{sd} - v_{cd} - v_{rd}) \\ \frac{di_{sq}}{dt} &= -\omega i_{sd} - \frac{r}{L}i_{sq} + \frac{1}{L}(v_{sq} - v_{cq} - v_{rq}) \end{aligned} \quad (3)$$

The matrix form of the dq axis can be rewritten as follows:

$$\frac{d}{dt} \begin{bmatrix} i_{sd} \\ i_{sq} \end{bmatrix} = \begin{bmatrix} -r/L & +\omega \\ -\omega & -r/L \end{bmatrix} \begin{bmatrix} i_{sd} \\ i_{sq} \end{bmatrix} + \frac{1}{L} \begin{bmatrix} v_{sd} - v_{cd} - v_{rd} \\ v_{sq} - v_{cq} - v_{rq} \end{bmatrix}$$

The modeling of the branch shunt: The mathematical model of the UPFC shunt is given similarly by the following equations:

$$\begin{aligned} \frac{di_{pa}}{dt} &= -\frac{r_p}{L_p}i_{pa} + \frac{1}{L_p}(v_{pa} - v_{ca} - v_{ra}) \\ \frac{di_{pb}}{dt} &= -\frac{r_p}{L_p}i_{pb} + \frac{1}{L_p}(v_{pb} - v_{cb} - v_{rb}) \\ \frac{di_{pc}}{dt} &= -\frac{r_p}{L_p}i_{pc} + \frac{1}{L_p}(v_{pc} - v_{cc} - v_{rc}) \end{aligned} \quad (4)$$

With a transformation park d, q researchers have the system of Eq. 5:

$$\begin{aligned} \frac{di_{pd}}{dt} &= ? i_{pq} - \frac{r_p}{L_p}i_{pd} + \frac{1}{L_p}(v_{pd} - v_{cd} - v_{rd}) \\ \frac{di_{pq}}{dt} &= -\omega i_{pd} - \frac{r_p}{L_p}i_{pq} + \frac{1}{L_p}(v_{pq} - v_{cq} - v_{rq}) \end{aligned} \quad (5)$$

The matrix form is given as follows:

$$\frac{d}{dt} \begin{bmatrix} i_{pd} \\ i_{pq} \end{bmatrix} = \begin{bmatrix} -r_p/L_p & -\omega \\ -\omega & -r_p/L_p \end{bmatrix} \begin{bmatrix} i_{pd} \\ i_{pq} \end{bmatrix} + \frac{1}{L_p} \begin{bmatrix} v_{pd} - v_{cd} - v_{rd} \\ v_{pq} - v_{cq} - v_{rq} \end{bmatrix}$$

The modeling of the UPFC branch continues: By passing on the principle of balance of power and neglecting the losses of the converters. The DC voltage V_{dc} by the following equation:

$$\frac{dv_c}{dt} = \frac{1}{CV_c}(p_e - p_{ep}) \quad (6)$$

Hence:

$$\begin{aligned} p_e &= v_{ca}i_{sa} + v_{cb}i_{sb} + v_{cc}i_{sc} \\ p_{ep} &= v_{pa}i_{pa} + v_{pb}i_{pb} + v_{pc}i_{pc} \end{aligned}$$

Where:

p_e = Active power consumption of the AC system

p_{ep} = Active power injected by the shunt inverter AC system

Applying the Park transformation on Eq. 6 researchers obtain:

$$\frac{dv_{dc}}{dt} = \frac{3}{2CV_{dc}}(v_{pd}i_{pd} + v_{pq}i_{pq} - v_{cd}i_{d} - v_{cq}i_{q}) \quad (7)$$

The UPFC series and shunt UPFC's are identical in every respect. The commands used to set the inverter are the same for the shunt inverter.

CONFIGURATION REGULATOR CIRCUIT

Theoretically, the UPFC should be treated as a multivariable system because both series and shunt converters are connected from one side to the transmission line and the other side in continuous DC circuit and thus each has two inputs and two outputs. This for to facilitate the synthesis of settings, treatment of the two converters will be done separately. The possibility of this separation is justified by two main factors.

First, the coupling between the two converters of the transmission line is quite small. Second, the dynamic variation of the voltage of DC side of the continuum is dominated by the parallel converter. Control of the converter in parallel UPFC is very similar to that of the compensator SVC.

So to control the flow of active power in the transmission line, the controller of the UPFC series must adjust the angle of the phase of the compensation voltage V_c while to adjust the flow of reactive power, the amplitude of the input voltage range must be controlled. To ensure system stability, a chain of control is implemented with PI control:

- Control of the series branch
- Control of parallel branch and the game continues

DESCRIPTION OF THE CONTROL SYSTEM OF UPFC

The active and reactive powers P and Q are given by the equations:

$$\begin{aligned} P &= \frac{3}{2} (V_{sd} \cdot i_{sd} + V_{sq} \cdot i_{sq}) \\ Q &= \frac{3}{2} (V_{sd} \cdot i_{sq} - V_{sq} \cdot i_{sd}) \end{aligned} \quad (8)$$

Where:

$$\begin{aligned} i_{rd} &= i_{sd} + i_{pd} \\ i_{rq} &= i_{sq} + i_{pq} \end{aligned}$$

Let the reference power and reactive P^* and Q^* of the desired real powers P and Q are used as input to the control system of UPFC. From Eq. 8, the reference currents i_{sd}^* and i_{sq}^* can be calculated as follows:

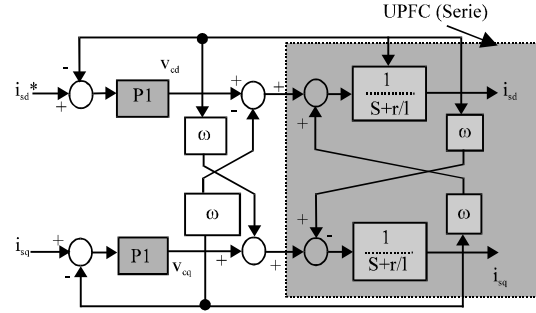


Fig. 3: Block diagram of the UPFC control (series)

$$i_{d}^* = \frac{2}{3} \left(\frac{P^* \cdot V_{sd} - Q^* \cdot V_{sq}}{\Delta} \right), \quad i_{q}^* = \frac{2}{3} \left(\frac{P^* \cdot V_{sq} + Q^* \cdot V_{sd}}{\Delta} \right)$$

With:

$$\Delta = V_{sd}^2 + V_{sq}^2 \quad (9)$$

The reference currents I_{rdref} I_{rqref} and are calculated according to Eq. 8. These reference values I_{rdref} and I_{rqref} are then compared with actual line currents from the receiver. The outputs of the PI editors provide the current values of control voltages V_{sd} and V_{cq} . The goal is to have active and reactive power at the finish line (Receiving end) identical to those instructions (P^* , Q^*) by forcing the line currents (I_{sd} , I_{sq}) to monitor properly their references.

The reference currents calculated (Eq. 8) compared to the actual line currents and after a correction to the current one ends control voltages (UPFC series) and V_{cd} , V_{cq} representing the reference voltage control circuit (PWM) of the inverter in Fig. 3.

DECOUPLED PI CONTROLLER

According to the system of Eq. 3 or 5, one can have the system contains a coupling between the reactive and active current I_d I_q . The interaction between current loops caused by the coupling term (ω) (Fig. 3). This explains the deviation of reactive power with respect to the reference. To reduce the interaction between the active and reactive power, a decoupling of the two current loops is needed.

The function of decoupling is to remove the product ωL and I_q controller along the axis d and adding the product term $\omega L I_d$ and the controller along the axis q. The design of the control system must begin with the selection of variables to adjust and then that of the control variables and their association with variables set.

There are various adjustment techniques well suited to the PI controller. There are two well-known empirical approaches proposed by Ziegler and Tit for determining the optimal parameters of the PI controller. The method Ziegler-Nichols used in the present thesis is based on a trial conducted in closed loop with a simple analog proportional controller.

The gain K_p of the regulator is gradually increased until the stability limit which is characterized by a steady oscillation.

Based on the results obtained, the parameters of the PI controller given by the analog transfer function:

$$K(s) = K_p \left(1 + \frac{1}{T_i s} \right)$$

Researchers can say in the conditions of the converter, the excess currents should be minimal. Therefore, the introduction of a simple condition $K_i = (r/L)k_p$. We obtain the transfer function $F(s) = k_p / (k_p s + 1)$ of the form is first class with a time constant:

$$T = 1/k_p$$

Hence:

$$F(s) = \frac{1}{1 + s.T} \quad (10)$$

Thus, determining the time constant depends on the maximum allowable change of control variables and V_{cd} , V_{cq} for controller series and the same for the shunt converter.

So according to the method of Ziegler-Nichols, the critical gain K_{pc} and the period T_c of the oscillations is measured by the choice of the table as follows:

$$K_p = 0.45k_{pc} \text{ and } T_i = 0.83, T_c \text{ avec } T_d = 0$$

SIMULATION RESULTS WITH PI-D UPFC

Figure 4a, b shows the behavior of active and reactive power where we see that the control system has a fast dynamic response to the forces reach their steady states after a change in the reference values. We also note the presence of the interaction between the two components (d and q).

These influences are caused by the PWM inverter is unable to produce continuous signals needed by the decoupling thus increasing the error in the PI-D controllers.

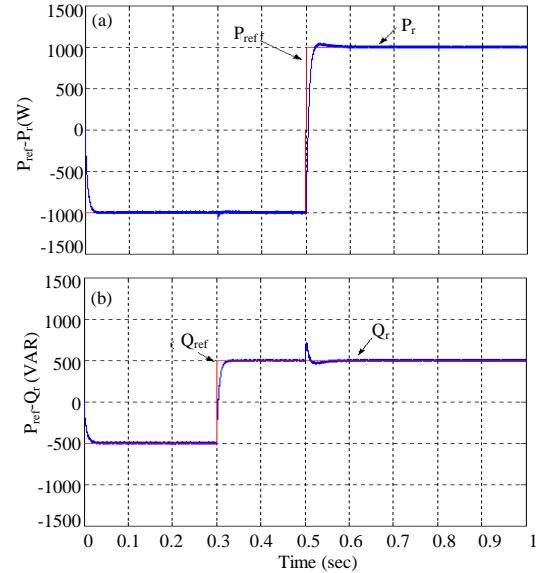


Fig. 4: Answers of powers with a PI-D

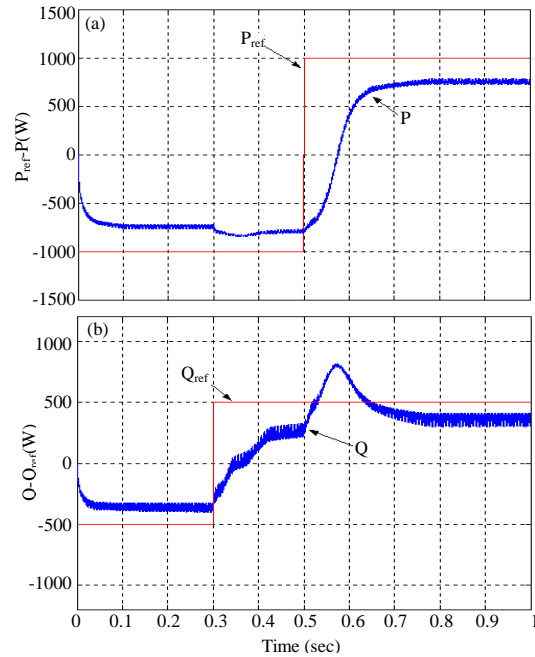


Fig. 5: Answers powers to change the reactance of 30%

To test robustness, we tested for a variation of the reactance XL to 30% and I had variations on the output power following. Following these changes, the active and reactive power (Fig. 5) undergo large deviations more or less with an overflow at times of great change instructions (P_{ref} , Q_{ref}) which means the performance degradation of the PI controller, interpreted by the loss of system stability. We simulated this time by introducing a perturbation (Fig. 6) duration of 25 m sec and amplitude

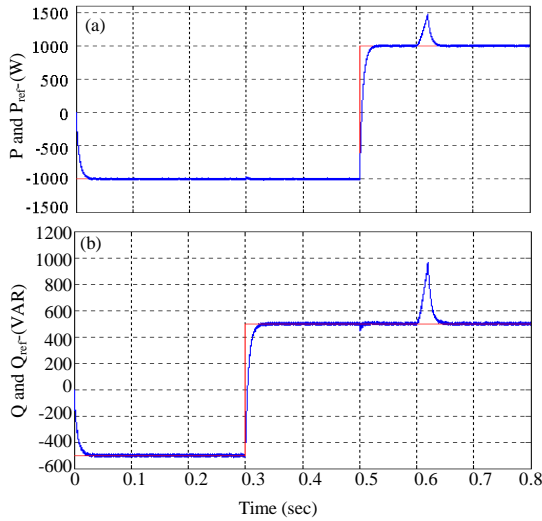


Fig. 6: UPFC system perturbed to test stability

1.5 to test again its robustness and stability of the system. The response of active and reactive power at 30% of XI could be detected; the error message given by Matlab command indicated the saturation of the order at infinity in the spikes of the reference signals. We can check the response of the servo not only continued but also regulation by adding a disturbance.

ADAPTIVE NEURAL CONTROL

The interest in adaptive control (Pages, 2001) appears mainly at the level of parametric perturbations, i.e. act on the characteristics of the process to be controlled, disturbance acting on the variables to control or order. In this study we present the method of adjustment proposed for the UPFC, emphasizing the classical approach based on neural networks.

CHOIX A NEURAL NETWORK

In this study, the Elman network (Li *et al.*, 2002) said hidden layer network is a recurrent network and therefore better suited for modeling dynamic systems. His choice in the neural control by state space is justified by the fact that in particular the network can be interpreted as a state space model nonlinear. Learning by back propagation algorithm standard is the law used for the identification of the UPFC.

STATE SPACE ADAPTIVE NEURAL CONTROL (SSNN)

The integration of these two approaches (neural adaptive control +) (Denai and Allaoui, 2002) in a single hybrid structure that each benefits from the other but to

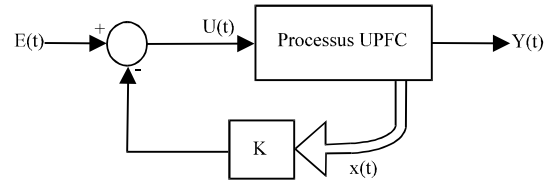


Fig. 7: Block diagram of a feedback control state of the UPFC

change the dynamic behavior of the UPFC system was added against a reaction calculated from the state vector (state space) (Fig. 7). The state feedback control is to consider the process model in the form of an equation of state:

$$X^*(t) = A.(t) + Bu(t) \tag{11}$$

And observation equation:

$$Y(t) = C.(t) + Du(t) \tag{12}$$

Where:

- u(t) = The control vector
- x(t) = The state vector
- y(t) = The output vector of dimension for a discrete system to the sampling process parameters Te at times of Te sample k are formalized as follows:

$$x(t+1) = A_d.(t) + Bu_d(t) \tag{13}$$

$$y(t) = C_d.(t) + D_d u(t) \tag{14}$$

The transfer function $G(s) = Y(s)/U(s)$ of the process UPFC can be written as:

$$G(s) = \frac{1}{s + r/L} \tag{15}$$

We deduce the equations of state representation of the UPFC:

$$\begin{cases} \dot{x}^* = -\left(\frac{r}{L}\right).x + u \\ y = x \end{cases} \tag{16}$$

With:

$$U(t) = e(t) - kx(t)$$

Let:

$$X(t+1) = [A_d - KB_d]x(t) + B_d e(t) \tag{17}$$

$$Y(t) = C_d x(t) \tag{18}$$

The dynamics of the process corrected by state space is presented based on the characteristic equation of the matrix $[A_d - B_d K]$ where, K is the matrix state space controlled process. The system is described in matrix form in the state space:

$$\begin{cases} \dot{x}^* = A.x + B.u \\ y = C.x + D.u \end{cases} \quad (19)$$

Where:

$$A = \begin{bmatrix} -\frac{r}{L} & \omega \\ -\omega & -\frac{r}{L} \end{bmatrix} \quad B = \begin{bmatrix} -\frac{1}{L} & 0 \\ 0 & -\frac{1}{L} \end{bmatrix} \quad C = \begin{bmatrix} 1 & 0 \\ 0 & 1 \end{bmatrix} \quad D = \begin{bmatrix} 0 & 0 \\ 0 & 0 \end{bmatrix}$$

$$u = \begin{bmatrix} v_{cd} \\ v_{cq} \end{bmatrix} \quad y = \begin{bmatrix} i_{sd} \\ i_{sq} \end{bmatrix} \quad x = [i_{sd} \quad i_{sq}]^T$$

IDENTIFICATION BASED NETWORK ELMAN

Process identified (Zebirate *et al.*, 2003; Zebirate and Chaker, 2003) will be characterized by the model structure (Fig. 8), of his order and parameter values. It is therefore, a corollary of the simulation process for which using a model and a set of coefficients to predict the response of the system. The Elman network consists of three layers; an input layer, hidden layer and output layer. The layers of input and output interfere with the external environment which is not the case for the intermediate layer called hidden layer ie the network input is the command $U(t)$ and its output is $Y(t)$.

The state vector $X(t)$ from the hidden layer is injected into the input layer. Researchers deduce the following equations:

$$X(t) = W_r X(t-1) + W_h U(t-1) \quad (20)$$

$$Y(t) = W_o X(t) \quad (21)$$

Where W_h , W_r and W_o are the weight matrices. Equations are standard descriptions of the state space of dynamical systems. The order of the system depends on the number of states equals the number of hidden layers. When an input-output data is presented to the network at iteration k^2 error at the output of the network is defined as:

$$E_t = \frac{1}{2} (y_d(t) - y(t))^2 \quad (22)$$

For all data $u(t)$, $y_d(t)$ de $t = 1, 2, \dots, N$, the sum of squared errors is:

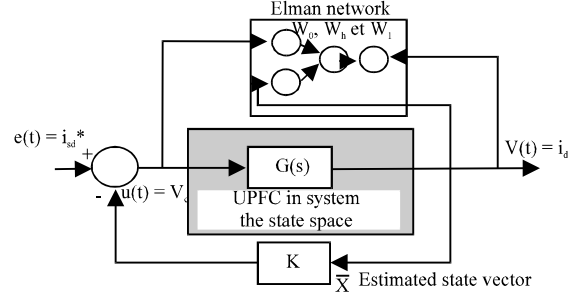


Fig. 8: Network ELMAN and state space

$$E = \sum_{t=1}^N E_t \quad (23)$$

The weights are modified at each iteration for W_o researchers have:

$$\begin{aligned} \frac{\partial E_t}{\partial W_o} &= -(y_d(t) - y(t)) \frac{\partial y(t)}{\partial W_o} \\ &= -(y_d(t) - y(t)) \cdot x^T(t) \end{aligned} \quad (24)$$

For W_h and W_r , were:

$$\begin{aligned} \frac{\partial E_t}{\partial W_h} &= -\frac{\partial E_t}{\partial y(t)} \cdot \frac{\partial y(t)}{\partial x(t)} \cdot \frac{\partial x(t)}{\partial W_h} \\ &= -(y_d(t) - y(t)) \cdot W_o^T \cdot u(t) \end{aligned} \quad (25)$$

$$\begin{aligned} \frac{\partial E_t}{\partial W_r^i} &= -\frac{\partial E_t}{\partial y(t)} \cdot \frac{\partial y(t)}{\partial x_1(t)} \cdot \frac{\partial x_1(t)}{\partial W_r^i} \\ &= -(y_d(t) - y(t)) \cdot W_o^i \cdot \frac{\partial x_1(t)}{\partial W_r^i} \end{aligned} \quad (26)$$

The latter we obtain:

$$\frac{\partial x_1}{\partial W_r^i} = X^T(t-1) + W_r^i \cdot \frac{\partial x(t-1)}{\partial W_r^i} \quad (27)$$

The variation of the weight matrix based on the learning gain is written as:

$$\Delta W = -\eta \cdot \frac{\partial E_t}{\partial W} \quad (28)$$

Note that the performance of the identification is better when the input signal is sufficiently high in frequency to excite the different modes of process. The three weights W_o , W_r and W_h which are, respectively the

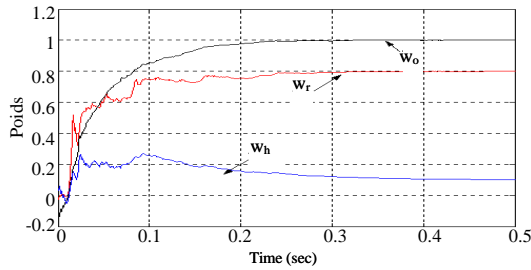


Fig. 9: Changing weight (Evolution des parametres (Poids)-SSNN)

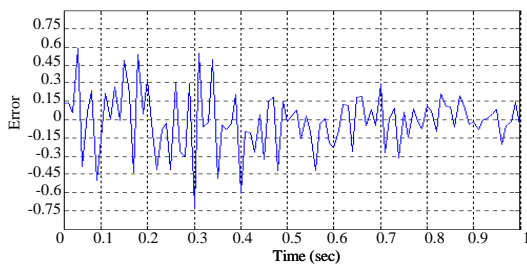


Fig. 10: Estimation error (SSNN)

matrices of the equation of state of the process system (UPFC) [CA and B] became stable after a rough time, $t = 0.3$ sec and several iterations (Fig. 9) (For the Elman network neuron type is assumed through the vector is zero ($D = 0$)).

In online learning Elman network, the task of identifying and correcting same synthesis are one after the other.

Or correction of the numerical values of the parameters is done repeatedly so the estimation error (Fig. 10) takes about almost a second ($t = 1$ sec) to converge to zero i_e regulation in pursuit.

ROBUSTNESS TEST

To check the robustness to the controller, two tests were performed. For each test we varied the parameters of the transmission line but the controller remains unchanged.

It can be seen that the variation of the reactance ($\pm 25\%$) has almost no influence on the output characteristics of the UPFC system (Fig. 11). To compare the responses of active and reactive power of UPFC system, researchers gave the three cases (Fig. 11) where (a) and (c) are the responses to changes ($\pm 25\%$) and (b) is the response of the system without any change in reactance.

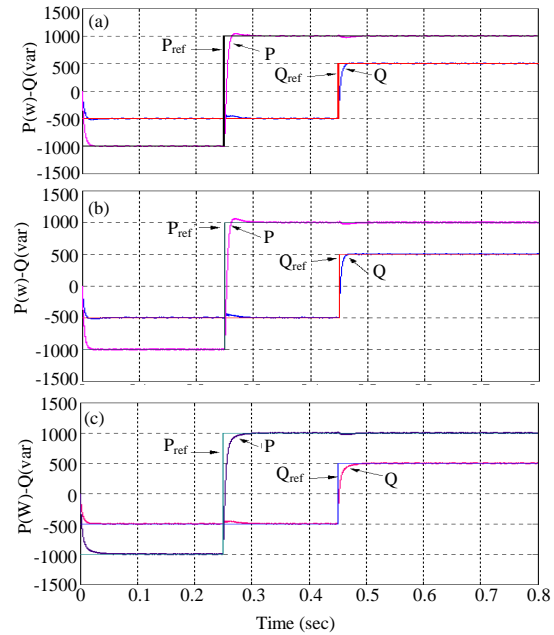


Fig. 11: Neural adaptive control (SSNN) Powers P, Q and at ($\pm 25\%$ XI)

CONCLUSION

The identification process will be characterized by the model structure, its order and parameter values. It is therefore, a corollary of the simulation process which uses a model and a set of coefficients to predict the response of the system. The use of more advanced low-identification neural network can be dependable in the calculation algorithm of the order. In this study, researchers used for the identification of system parameters a neuron network said Elman network with three layers.

Note that the performance of the identification is better when the input signal is sufficiently high in frequency to excite the different modes of process. Neural adaptive control by state feedback (SSNN: State Space Neural Network) is a hybrid control based on the representation of system status UPFC was tested. The performance of the latter are slightly degraded, this is may be due to the delay caused by the algorithm, it can not be reduced at will or it may due to the choice of the gain K of the closed loop.

Finally, the identification process based on learning of Elman neural network, provides the dynamic behavior of the process and to estimate the system output as its state vector based on the information that are control signal and the measured output.

REFERENCES

- Denai, M.A. and T. Allaoui, 2002. Adaptive fuzzy decoupling of UPFC-power flow compensation. Proceedings of the 37th UPEC2002, September 9-11, 2002, Staffordshires University, UK -
- Gyugyi, L., 1992. Unified power flow control concept for flexible AC transmission systems. IEE Proc., 139: 323-331.
- Li, X., G. Chen, Z. Chen and Z. Yuan, 2002. Chaotifying linear elman networks. IEEE Trans. Neural Networks, 3: 1193-1199.
- Pages, O., 2001. Etude de comparaison de differentes structures de commande multi- controleurs application a un axe robotise. Ph.D. These, (LAMII/CESALP), Universite de Savoie, France.
- Papic, I., P. Zunko, D. Povh and M. Weinhold, 1997. Basic control of unified power flow controller. IEEE Trans. Power Syst., 12: 1734-1739.
- Song, Y.H. and A.T. Johns, 1999. Flexible AC Transmission System (FACTS). Volume 30 of IEE Power and Energy Series, The Institute of Electrical Engineers, London, ISBN: 9780852967713, Pages: 592.
- Zebirate, S. and A. Chaker, 2003. Commande addaptative decouple neuronale d'un UPFC (unified power flow control). JCGE Saint Nazaire, Juin 2003.
- Zebirate, S., A. Chaker and O. Traiaia, 2003. Commande addaptative decouple neuronale d'un compensateur de flux de puissance UPFC' reference 480. Laboratoire LAAS.CCECE 03-CCGEI 2003. Montreal. IEEE May 2003.